Entanglement driven phase transitions in spin-orbital models

Wen-Long You[1,2], **Andrzej M. Oleś**[1,3] **and Peter Horsch**[1]

[1] Max-Planck-Institut für Festkörperforschung,
Heisenbergstrasse 1, D-70569 Stuttgart, Germany
[2] College of Physics, Optoelectronics and Energy, Soochow University,
Suzhou, Jiangsu 215006, People's Republic of China
[3] Marian Smoluchowski Institute of Physics, Jagiellonian University,
prof. S. Łojasiewicza 11, PL-30348 Kraków, Poland

E-mail: a.m.oles@fkf.mpg.de

Abstract. To demonstrate the role played by the von Neumann entropy spectra in quantum phase transitions we investigate the one-dimensional anisotropic SU(2)$\otimes XXZ$ spin-orbital model with negative exchange parameter. In the case of classical Ising orbital interactions we discover an unexpected novel phase with Majumdar-Ghosh-like spin-singlet dimer correlations triggered by spin-orbital entanglement and having $k = \pi/2$ orbital correlations, while all the other phases are disentangled. For anisotropic XXZ orbital interactions both spin-orbital entanglement and spin-dimer correlations extend to the antiferro-spin/alternating-orbital phase. This quantum phase provides a unique example of two coupled order parameters which change the character of the phase transition from first-order to continuous. Hereby we have established the von Neumann entropy spectral function as a valuable tool to identify the change of ground state degeneracies and of the spin-orbital entanglement of elementary excitations in quantum phase transitions.

PACS numbers: 75.25.Dk, 03.67.Mn, 05.30.Rt, 75.10.Jm

Submitted to: *New J. Phys.*

1. Spin-orbital physics and von Neumann entropy spectra

In the Mott-insulating limit of a transition metal oxide the low-energy physics can be described by Kugel-Khomskii-type models [1], where both spin and orbital degrees of freedom undergo joint quantum fluctuations and novel types of spin-orbital order [2] or disorder [3] may emerge. Following the microscopic derivation from the multiorbital Hubbard model, the generic structure of spin-orbital superexchange takes the form of a generalized Heisenberg model [4, 5],

$$H = \sum_{\langle ij\rangle\parallel\gamma} \left\{ J_{ij}^{(\gamma)}(\vec{T}_i,\vec{T}_j)\vec{S}_i\cdot\vec{S}_j + K_{ij}^{(\gamma)}(\vec{T}_i,\vec{T}_j) \right\}, \tag{1}$$

as indeed found not only for the simplest systems with $S = 1/2$ spins: $KCuF_3$ [1], the $RTiO_3$ perovskites [6], $LiNiO_2$ and $NaNiO_2$ [7], Sr_2CuO_3 [8], or alkali RO_2 hyperoxides [9], but also for larger spins as e.g. for $S = 2$ in $LaMnO_3$ [10]. In such models the parameters that determine the spin-S Heisenberg interactions stem from orbital operators $J_{ij}^{(\gamma)}$ and $K_{ij}^{(\gamma)}$ — they depend on the bond direction and are controlled by the orbital degree of freedom which is described by pseudospin operators $\{\vec{T}_i\}$. That is, these parameters are not necessarily fixed by rigid orbital order [3, 11], but quantum fluctuations of orbital occupation [12, 13] may strongly influence the form of the orbital operators, particularly in states with spin-orbital entanglement (SOE) [14, 15]. As a consequence, amplitudes and even the signs of the effective exchange can fluctuate in time. Such entangled spin-orbital degrees of freedom can form new states of matter, as for instance the orbital-Peierls state observed at finite temperature in YVO_3 [16, 17]. Another example are the collective spin and orbital excitations in a one-dimensional (1D) spin-orbital chain under a crystal field which can be universally described by fractionalized fermions [18]. It is challenging to ask which measure of SOE would be the most appropriate one to investigate quantum phase transitions in such systems.

The subject is rather general and it has become clear that entanglement and other concepts from quantum information provide a useful perspective for the understanding of electronic matter [19–23]. Other examples of entangled systems are: topologically nontrivial states [24], relativistic Mott insulators with $5d$ ions [25], ultracold alkaline-earth atoms [26], and skyrmion lattices in the chiral metal MnSi [27].

One well-known characterization of a quantum system is the entanglement entropy (EE) determined by bipartitioning a system into A and B subsystems. This subdivision can refer for example to space [19, 28], momentum [28, 29], or different degrees of freedom such as spin and orbital [30]. A standard measure is the von Neumann entropy (vNE), $\mathcal{S}^0_{\rm vN} \equiv -{\rm Tr}_A\{\rho^0_A \log_2 \rho^0_A\}$, for the ground state $|\Psi_0\rangle$ which is obtained by integrating the density matrix, $\rho^0_A = {\rm Tr}_B|\Psi_0\rangle\langle\Psi_0|$, over subsystem B. Another important measure is the entanglement spectrum (ES) introduced by Li and Haldane [31], which has been explored for gapped 1D spin systems [32], quantum Heisenberg ladders [33], topological insulators [34], bilayers and spin-orbital systems [28]. The ES is a *property of the ground state* and basically represents the eigenvalues p_i of the reduced density matrix ρ^0_A obtained by bipartitioning of the system. Interestingly

a correspondence of the ES and the tower of excitations relevant for SU(2) symmetry breaking has been pointed out recently [35]. It was also noted that the ES can exhibit singular changes, although the system remains in the same phase [36]. This suggests that the ES has less universal character than initially assumed [37].

In this paper we explore a different entanglement measure, namely the vNE spectrum which monitors the vNE of ground and *excited states* of the system, for instance of a spin-orbital system as defined in equation (1). In this case we consider the entanglement obtained from the bipartitioning into spin and orbital degrees of freedom in the entire system [30]. Here the vNE is obtained from the density matrix, $\rho_s^{(n)} = \mathrm{Tr}_o|\Psi_n\rangle\langle\Psi_n|$, by taking the trace over the orbital degrees of freedom (Tr_o) for each eigenstate $|\Psi_n\rangle$. We show below that the vNE spectrum,

$$\mathcal{S}_{\mathrm{vN}}(\omega) = -\sum_n \mathrm{Tr}_s\{\rho_s^{(n)} \log_2 \rho_s^{(n)}\}\delta\left\{\omega - \omega_n\right\}, \tag{2}$$

reflects the changes of SOE entropy for the different states at phase transitions. The excitation energies, $\omega_n = E_n - E_0$, of eigenstates $|\Psi_n\rangle$ are measured with respect to the ground state energy E_0. It has already been shown that the vNE spectra uncover a surprisingly large variation of entanglement within elementary excitations [30]. Also certain spectral functions have been proposed, that can be determined by resonant inelastic x-ray scattering [38], and provide a measure of the vNE spectral function. Here we generalize this function to arbitrary excitations $|\Psi_n\rangle$, i.e., *beyond* elementary excitations which refer to a particular ground state. We demonstrate that focusing on general excited states opens up a new perspective that sheds light on quantum phase transitions and the entanglement in spin-orbital systems.

The paper is organized as follows: In section 2 we introduce the 1D spin-orbital model with ferromagnetic exchange, and in section 3 we present its phase diagrams for the Ising limit of orbital interactions and for the anisotropic SU(2)$\otimes XXZ$ model with enhanced Ising component. SOE is analyzed in section 4 using both the spin-orbital correlation function and the entanglement entropy and we show that these two measures are equivalent. In section 5 we present the entanglement spectra and discuss their relation to the quantum phase transitions. The main conclusions and summary are given in section 6. The distance dependence of spin correlations in the antiferromagnetic phase is explored in the Appendix.

2. Ferromagnetic SU(2)$\otimes XXZ$ spin-orbital model

The motivation for our theoretical discussion of spin-orbital physics comes from t_{2g} electron systems in which orbital quantum fluctuations are enhanced by an intrinsic reduction of the dimensionality of the electronic structure [12]. Examples of strongly entangled quasi-1D t_{2g} spin-orbital systems due to dimensional reduction are well known and we mention here just $LaTiO_3$ [6], $LaVO_3$ and YVO_3 [13], where the latter two involve $\{yz, zx\}$ orbitals along the c cubic axis; as well as p_x and p_y orbital systems in 1D fermionic optical lattices [39–41]. This motivates us to consider the 1D spin-orbital

model for $S = 1/2$ spins and $T = 1/2$ orbitals with anisotropic XXZ interaction, i.e., with reduced quantum fluctuation part in orbital interactions. The $|+\rangle$ and $|-\rangle$ orbital states are a local basis at each site and play a role of yz and zx states in t_{2g} systems,

$$\mathcal{H}(x,y,\Delta) \;=\; -\,J\sum_{j=1}^{L}\Big(\vec{S}_j\cdot\vec{S}_{j+1}+x\Big)\Big([\vec{T}_j\cdot\vec{T}_{j+1}]_\Delta+y\Big)\,, \tag{3}$$

$$[\vec{T}_j\cdot\vec{T}_{j+1}]_\Delta \equiv \Delta\left(T_j^xT_{j+1}^x+T_j^yT_{j+1}^y\right)+T_j^zT_{j+1}^z, \tag{4}$$

where $J>0$ and we use periodic boundary conditions for a ring of L sites, i.e., $L+1\equiv 1$. The parameters of this model are $\{x,y\}$ and Δ. At $x=y=1/4$ and $\Delta=1$ the model has SU(4) symmetry. Hund's exchange coupling does not only modify x and y but also leads to the XXZ anisotropy ($\Delta<1$), a typical feature of the orbital sector in real materials [5, 12]. The antiferromagnetic model ($J=-1$) is Bethe-Ansatz integrable at the SU(4) symmetric point [42] and its phase diagram is well established by numerical studies [43, 44]. It includes two phases with dimer correlations [45] which arise near the SU(4) point. Some of its ground states could be even determined exactly at selected (x,y,Δ) points [46–50].

Here we are interested in the complementary and less explored model with negative (ferromagnetic) coupling ($J=1$), possibly realized in multi-well optical lattices [51], which has been studied so far only for SU(2) orbital interaction ($\Delta=1$) [30]. This model is physically distinct from the antiferromagnetic ($J=-1$) model, except for the Ising limit ($\Delta=0$) where the two models can be mapped onto each other, but none was investigated so far. The phase diagrams for $J=1$, see figure 1, determined using the fidelity susceptibility [52] display a simple rule that the vNE (2) vanishes for exact ground states of rings of length L which can be written as products of spin ($|\psi_s\rangle$) and orbital ($|\psi_o\rangle$) part, $|\Psi_0\rangle = |\psi_s\rangle\otimes|\psi_o\rangle$.

3. Phase transitions in the spin-orbital model

To understand the role played by the SOE in the 1D spin-orbital model (3) and (4) we consider the phase diagrams for $\Delta=0$ and $\Delta=0.5$, see figure 1. In the case $\Delta=0$ all trivial combinations of ferro (F) and antiferro (A) spin-orbital phases labeled I-IV have $\mathcal{S}^0_{\rm vN}=0$, i.e., spins and orbitals disentangle in all these ground states: FS/FO, AS/FO, AS/AO, FS/AO. If both subsystems exhibit quantum fluctuations, the ground state $|\Psi_0\rangle$ can no longer be written in the product form. This occurs for the AS/AO phase III at $\Delta>0$.

Most remarkable is the strongly entangled phase V at $\Delta=0$ and $y<0$, see figure 1(a). This phase occurs near $x\simeq -\langle\vec{S}_j\cdot\vec{S}_{j+1}\rangle_{\rm AF}\equiv \ln 2-1/4$, i.e., when the uniform antiferromagnetic spin correlations in phase III are compensated by the parameter x, so that the energy associated with Hamiltonian (3) *de facto disappears*. This triggers state V with strong SOE (see below) as the only option for the system to gain substantial energy in this parameter range by nonuniform spin-orbital correlations. The analysis of

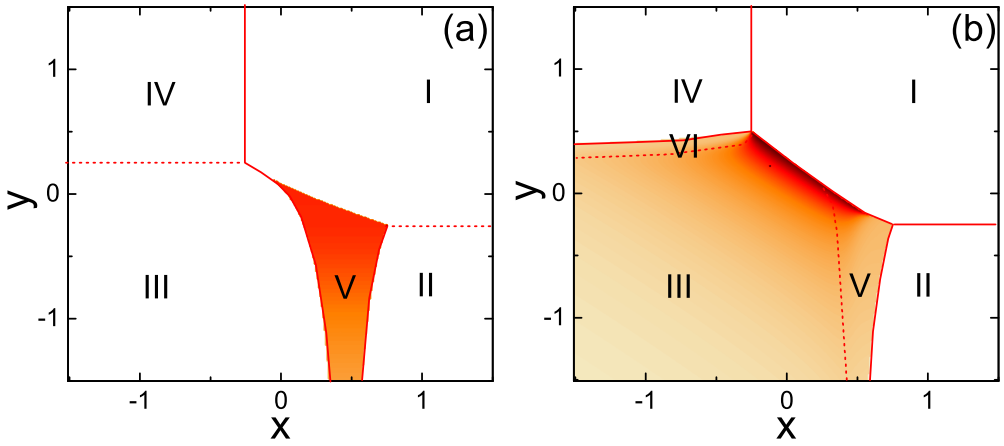

Figure 1. Phase diagrams of the spin-orbital model [equation (3)] obtained by two methods, fidelity susceptibility or an exact diagonalization of an $L = 8$ site model, for: (a) $\Delta = 0$, and (b) $\Delta = 0.5$. The spin-orbital correlations in phases I-IV correspond to FS/FO, AS/FO, AS/AO, FS/AO order (see text). At $\Delta = 0$ only the ground state of a novel phase V has finite EE, $\mathcal{S}^0_{\rm vN} > 0$ (shaded), whereas at $\Delta > 0$ the EE in phases III and VI is also finite.

phase V in terms of the longitudinal equal-time spin (orbital) structure factors

$$O^{zz}(k) = \frac{1}{L^2} \sum_{m,n=1}^{L} e^{-ik(m-n)} \langle O^z_m O^z_n \rangle, \tag{5}$$

where $O = S$ or T, reveals in figure 2(a) at $\Delta = 0$ and $y = -1/4$ for the spin structure factor $S^{zz}(k) \propto (1 - \cos k)$. This is a manifestation of nearest neighbour correlations, while further neighbour spin correlations vanish and moreover we find a quadrupling in the orbital sector, see figure 2(b). Thus the spin correlations indicate either a short-range spin liquid or a translational invariant dimer state.

The *hidden spin-dimer order* [53] can be detected by the four-spin correlator (we use periodic boundary conditions),

$$D(r) = \frac{1}{L} \sum_{j=1}^{L} \left[\left\langle (\vec{S}_j \cdot \vec{S}_{j+1})(\vec{S}_{j+r} \cdot \vec{S}_{j+1+r}) \right\rangle - \left\langle \vec{S}_j \cdot \vec{S}_{j+1} \right\rangle^2 \right]. \tag{6}$$

At $\Delta = 0$ we find $|D(r)|$ with long-range dimer correlations in phase V, but not in III. Phase III is a state with alternating ($k = \pi$) spin (orbital) correlations in the range $x < 0.17$ shown in figures 2(a,b). Interestingly for $\Delta > 0$ the dimer spin correlations $|D(r)|$ are not only present in phase V but also appear in phase III. Moreover a phase VI emerges, complementary to phase V, with interchanged role of spins and orbitals, see figure 1(b). The order parameters for phase VI follow from the form of structure factors which develop similar but complementary momentum dependence to that for phase V seen in figure 2(a), i.e., maxima at $\pi/2$ for $S^{zz}(k)$ and at π for $T^{zz}(k)$. We remark that phases V and VI are unexpected and they were overlooked before for the SU(2)⊗SU(2) model at $\Delta = 1$ [30]. From the size dependence of $|D(r)|$ in figures 2(c,d) we conclude

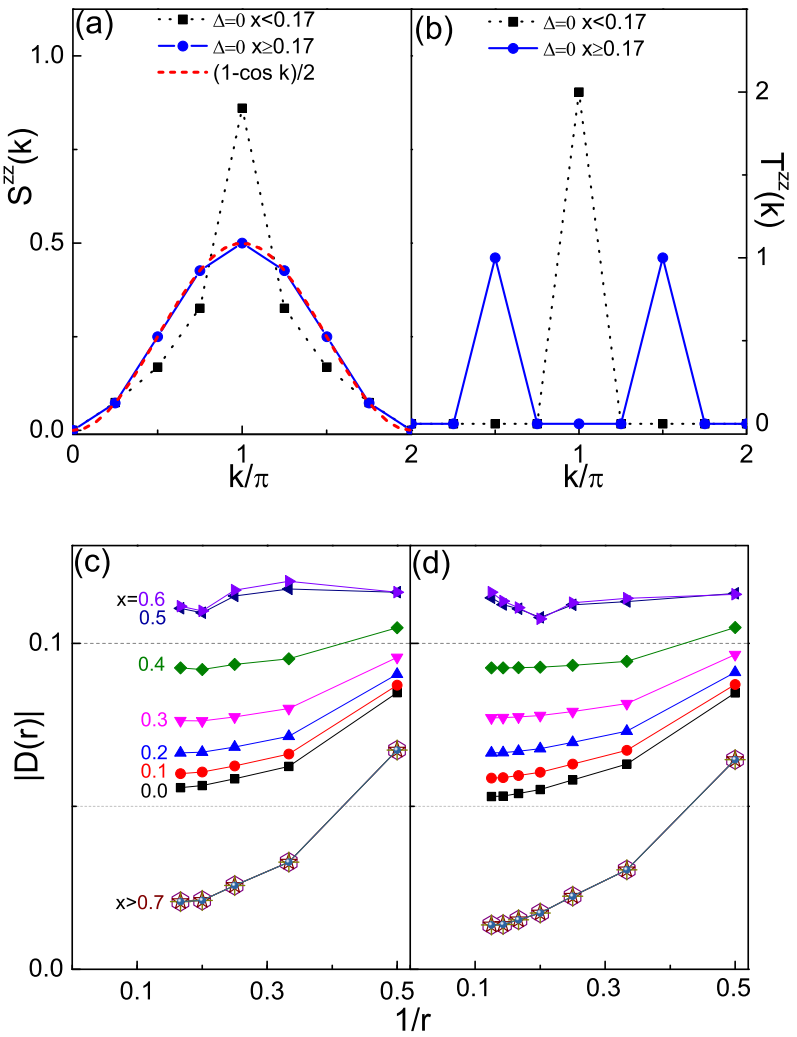

Figure 2. Top— Spin $[S^{zz}(k)]$ and orbital $[T^{zz}(k)]$ structure factors (5) for the 1D spin-orbital model (3) of $L = 8$ sites at $\Delta = 0$ and $y = -1/4$: (a) $S^{zz}(k)$ and (b) $T^{zz}(k)$. Bottom— Spin dimer correlations $D(r)$ equation (6) found at $\Delta = 0.5$ for decreasing $1/r$ for clusters of (c) $L = 12$ and (d) $L = 16$ sites.

that the dimer correlations are long-ranged at $\Delta = 0.5$ in phase V, but also in III, as seen from the data for $x \in [0.0, 0.4)$, where they coexist with the AS correlations.

These results suggest that the ground state V in figure 1(a) is formed by spin-singlet product states

$$|\Phi_1^D\rangle = [1,2][3,4][5,6]\cdots[L-1,L],$$
$$|\Phi_2^D\rangle = [2,3][4,5][6,7]\cdots[L,1], \qquad (7)$$

where $[l, l+1] = (|\uparrow\downarrow\rangle - |\downarrow\uparrow\rangle)/\sqrt{2}$ denotes a spin singlet. They are not coupled to orbital singlets on alternating bonds as it happens for the AFantiferromagnetic SU(2)⊗SU(2) spin-orbital chain in a different parameter regime [46], but to Ising configurations in the

orbital sector. The four-fold ($k = \pi/2$) periodicity of orbital correlations is consistent with four orbital states:

$$
\begin{aligned}
|\Psi_1^z\rangle &= |++--++\cdots--\rangle,\\
|\Psi_2^z\rangle &= |-++--+\cdots+-\rangle,\\
|\Psi_3^z\rangle &= |--++--\cdots++\rangle,\\
|\Psi_4^z\rangle &= |+--++-\cdots-+\rangle.
\end{aligned}
\tag{8}
$$

The decoupling of singlets is complete for $y = -1/4$ and $\Delta = 0$, where $(++)$ and $(--)$ bonds yield vanishing coupling in equation (3), and the phase boundaries of region V are $x^c_{\rm III,V} = 3/4 + 2\langle \vec{S}_j \cdot \vec{S}_{j+1}\rangle_{\rm AF} \simeq 0.136$ and $x^c_{\rm V,II} = 3/4$ in the thermodynamic limit; moreover we find perfect long-range order of spin singlets, i.e., $D(r) = (3/8)^2(-1)^r$.

The dimerized spin-singlet state at $\Delta = 0$ has the same spin structure as the Majumdar-Ghosh (MG) state [54], however its origin is different. While the MG state in a J_1-J_2 Heisenberg chain results from frustration of antiferromagnetic exchange (at $J_2 = J_1/2$), here the spin singlets are induced by the SOE. At $\Delta = 0$ the only phase with finite SOE $\mathcal{S}^0_{\rm vN} = 1$ is phase V, see figure 3. In contrast, for $\Delta > 0$ one finds finite EE also in phase III, when the original product ground state changes into a more complex superposition of states and joint spin-orbital fluctuations [14] appear. These correlations control the SOE and give equivalent information to $\mathcal{S}^0_{\rm vN}$, see section 4. Furthermore, EE increases with x towards phase V where it is further amplified and exceeds $\mathcal{S}^0_{\rm vN} = 1$. The related softening of orbital order will be discussed below. Interestingly we find a one-to-one correspondence of finite EE and long-range order in the spin dimer correlations

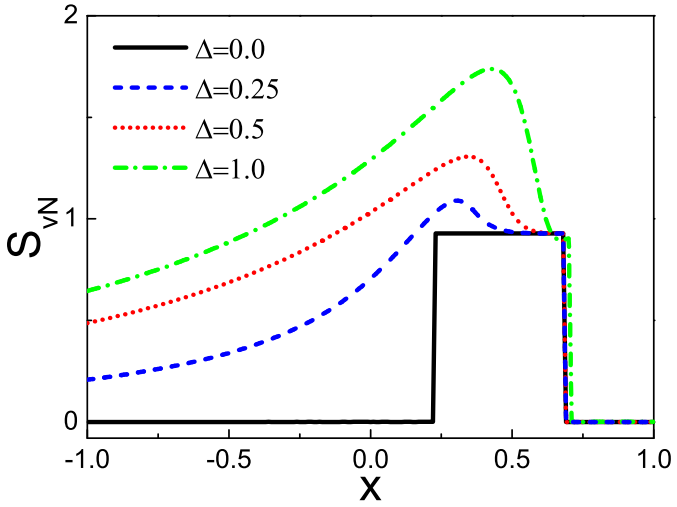

Figure 3. Spin-orbital entanglement entropy $\mathcal{S}^0_{\rm vN}$ in the ground state of the spin-orbital model (3) for the three phases III, V and II as a function of x for various Δ. Solid line for $\Delta = 0$ stands for the $k = 0$ ground state in the limit of $\Delta \to 0$. Parameters: $y = -0.5$ and $L = 8$.

$|D(r)|$.

The superstructure of phase V emerges from the interplay of spin and orbitals, where orbitals modulate the interaction of spins in equation (3), and *vice versa*. It is important to distinguish this from the Peierls effect, where the coupling to the lattice is an essential mechanism. The orbital Peierls effect observed in vanadates [16, 17] or the orbital-selective Peierls transition studied recently [55] fall into the former category, yet, as they involve orbital singlets — they are distinct from the case discussed here.

4. Spin-orbital entanglement

The description of spin-orbital entanglement in terms of the vNE entropy, as discussed in section 3, is a very convenient measure of entanglement. But it is also a highly abstract measure. To capture its meaning, one has to refer to mathematical intuition, namely to the fact that any product state, $|\Psi\rangle = |\psi_s\rangle \otimes |\psi_o\rangle$, has zero vNE. That is, an entangled state is a state that cannot be written as a single product. A more physical measure are obviously spin-orbital correlation functions relative to their mean-field value [14]. Such correlation functions vanish for product states where mean-field factorization of the relevant product is exact, i.e., spins and orbitals are disentangled.

To detect spin-orbital entanglement in the ground state we evaluate here the joint spin-orbital bond correlation function C_1 for the SU(2)$\otimes XXZ$ model (3), defined as follows for a nearest neighbour bond $\langle i, i+1\rangle$ in the ring of length L [14],

$$C_1 \equiv \frac{1}{L}\sum_{i=1}^{L}\Big\{\Big\langle(\vec{S}_i\cdot\vec{S}_{i+1})(\vec{T}_i\cdot\vec{T}_{i+1})\Big\rangle - \Big\langle\vec{S}_i\cdot\vec{S}_{i+1}\Big\rangle\Big\langle\vec{T}_i\cdot\vec{T}_{i+1}\Big\rangle\Big\}. \tag{9}$$

The conventional intersite spin- and orbital correlation functions are:

$$S_r \equiv \frac{1}{L}\sum_{i=1}^{L}\Big\langle\vec{S}_i\cdot\vec{S}_{i+r}\Big\rangle, \tag{10}$$

$$T_r \equiv \frac{1}{L}\sum_{i=1}^{L}\Big\langle\vec{T}_i\cdot\vec{T}_{i+r}\Big\rangle. \tag{11}$$

The above general expressions imply averaging over the exact (translational invariant) ground state found from Lanczos diagonalization of a ring. While S_r and T_r correlations indicate the tendency towards particular spin and orbital order, C_1 quantifies the spin-orbital entanglement — if $C_1 \neq 0$ spin and orbital degrees of freedom are entangled and the mean-field decoupling in equation (3) cannot be applied as it generates uncontrollable errors.

Figures 4(a) and 4(b) show the nearest neighbour correlation functions S_1, T_1 and C_1 at $y = -0.5$, for $\Delta = 0$ and $\Delta = 0.5$, respectively, as functions of x. The nearest neighbour spin correlation function S_1 is antiferromagnetic (negative) in all phases III, V and II shown in figure 4, while (*negative*) T_1 indicates AO correlations in phase III and ferro-orbital (*positive*) in phase II. Finite $\Delta = 0.5$ triggers orbital fluctuations which

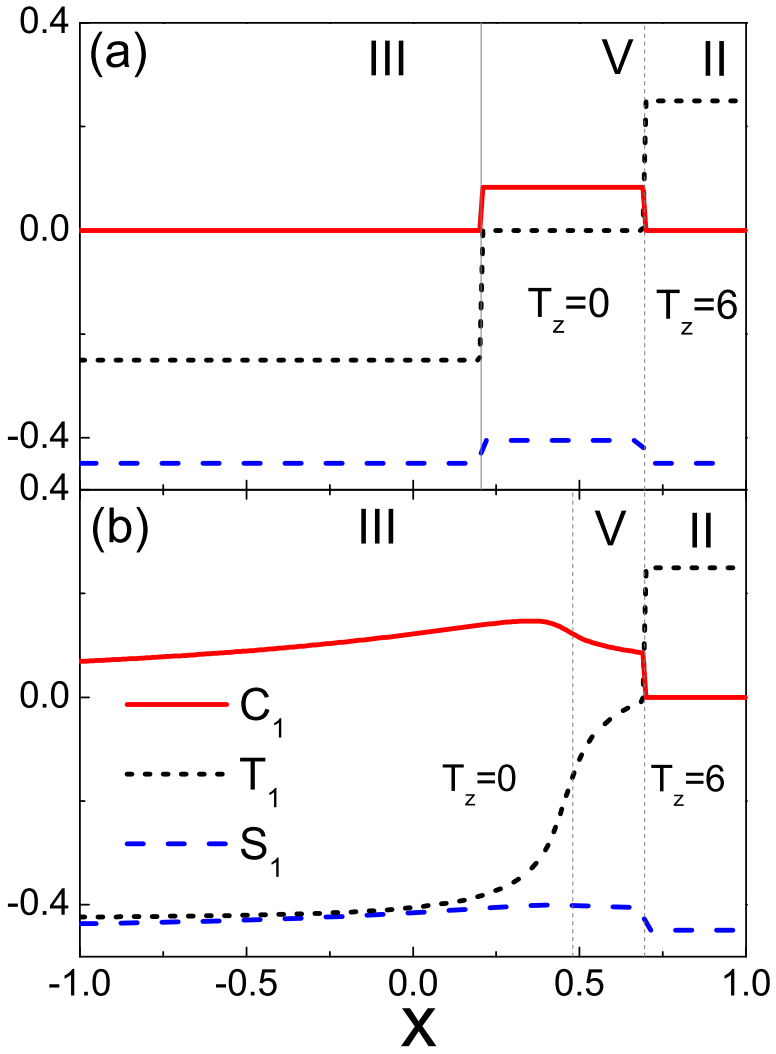

Figure 4. Nearest neighbour spin S_1 (10), orbital T_1 (11), and joint spin-orbital C_1 (9) correlations as obtained for a spin-orbital ring (3) with $L = 12$ sites and $y = -0.5$, as functions of x for: (a) $\Delta = 0$, and (b) $\Delta = 0.5$. The III-V phase boundary (dotted vertical line) in (b) has been determined by the maximum of the fidelity susceptibility [52].

lower T_1 below the classical value of 0.25 found at $\Delta = 0$. In the intermediate spin dimer phase T_1 is negative for all $\Delta > 0$, while it is zero for $\Delta = 0$.

It is surprising that C_1 is positive in phase V at $\Delta = 0$ in spite of the classical Ising orbital interactions, see figure 4(a). It is also positive in phases III and V at $\Delta = 0.5$ [see figure 4(b)]. Note that *positive* C_1 is found in the present spin-orbital chain with $J > 0$, while C_1 is *negative* when $J < 0$ [42]. In phase II C_1 vanishes in the entire parameter range as then the ground state can be written as a product. The same is true for phase III at $\Delta = 0$. We emphasize that the dependence of C_1 on x is completely analogous to that of the von Neumann entropy in figure 3, which also displays a broad maximum in the vicinity of the III-V phase transition at $\Delta = 0.5$, and a step-like structure in phase V

at $\Delta = 0$. Thus we conclude here that the vNE yields a faithful measure of SOE in the ground state that is qualitatively *equivalent* to the more direct entanglement measure via the spin-orbital correlation function C_1 [14].

5. Entanglement spectra and quantum phase transitions

Figure 3 stimulates the question about the origin and the understanding of the sudden or gradual EE changes at phase transitions. This can be resolved by exploring the vNE spectral function defined in equation (2) and shown in figures 5(a) and 5(b) for $\Delta = 0$ and 0.5, where colors encode the vNE of states. The excitation energies $\omega_n(x) = E_n(x) - E_0(x)$ are plotted here as function of the parameter x. Only the lowest excitations are shown that are relevant for the phase transitions and the low-temperature physics. They include: (i) the elementary excitations of the respective ground state, and (ii) the many-body excited states that are relevant for the phase transition(s) and may become ground states or elementary excitations in neighbouring phases when the parameter x is varied.

The AS/FO ground state of phase II in figure 5(a) obtained for a ring of $L = 8$ sites is an AS singlet ($S = 0$) with a maximal orbital quantum number, $T = L/2 = 4$, and a twofold ($k = 0, \pi$) degeneracy at $\Delta = 0$. The spin excitation spectrum appears as horizontal (red) lines and consists of gapless triplet $S = 1$ excitations. The low-lying excitations of the Bethe-Ansatz-solvable antiferromagnetic Heisenberg chain form a two-spinon (s-$\bar{s}$) continuum, whose lower bound is given by $\varepsilon(k) = \pi|\sin k|/2$ in the thermodynamic limit [56]. For the $L = 8$ ring the spectrum is discrete with a $\Delta k = \pi/4$ spacing, and it is known that the energy of triplet excitations $\varepsilon^S(\pi)$ will scale to zero as $1/L$ [57–59]. Red lines in phase II with finite slope are orbital excitations. The x-dependence is due to the spin part of $\mathcal{H}$ (3) which determines both the orbital energy scale and the dispersion, $J_T \equiv (x + \langle \vec{S}_j \cdot \vec{S}_{j+1} \rangle_{\rm AF})(1 - \Delta \cos k)$. This energy changes with x and at finite Δ also with momentum k, see figure 5(b). While the orbitons are gapped, the low-lying excitations are either magnons or x-dependent spin-orbital excitations. It is remarkable that the latter are entangled in general, although the ground state II is disentangled.

With decreasing x a first-order phase transition from II to V occurs by level crossing of disentangled (red) and entangled (green) ground states. The spin-singlet ($S = 0$) ground state of phase V has degeneracy 4 at $\Delta = 0$, and its components are labeled by the momenta $k = 0, \pm\pi/2, \pi$. This is reflected by finite φ^T order parameter in figure 6(a). Note that at $\Delta > 0$ this four-fold ground state degeneracy is lifted. In the spin-dimer phase a gap opens in the spectrum of elementary spin excitations [60, 61]. The one-magnon triplet gap $\Delta_S(\delta) \propto \delta^{3/4}$ depends on y via the dimerization parameter $\delta \equiv 1/|4y|$. In phase V even the pure magnetic excitations are entangled [see horizontal green lines in figure 5(a)]. The lowest excitations in the vicinity of the phase transitions have orbital character. From finite EE in figure 5(a) one recognizes that these states are inseparable spin-orbital excitations.

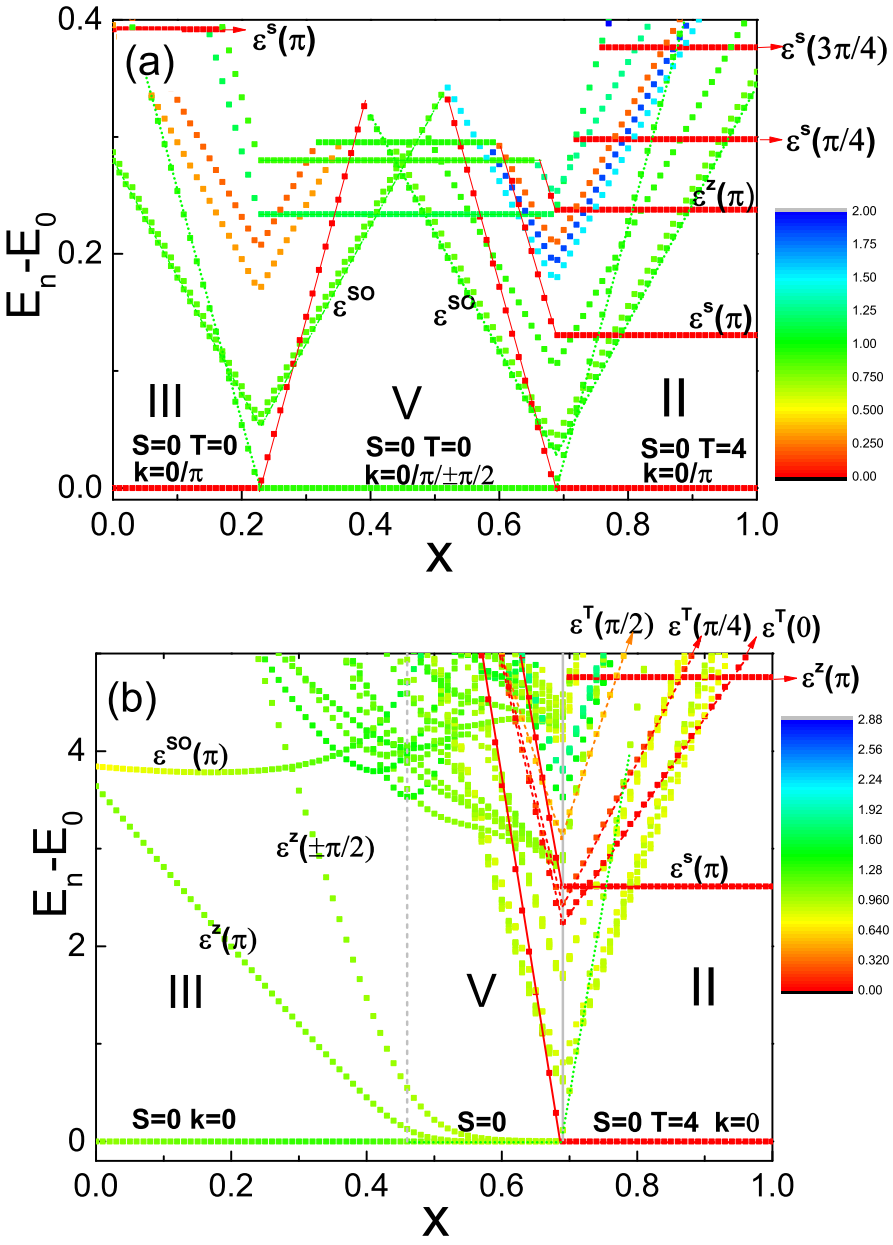

Figure 5. vNE-spectrum of lowest energies $E_n(x)$ (relative to the ground state energy $E_0(x)$) versus x with colors representing the size of the vNE of individual states. Data for the three phases III, V and II is shown for $y = -0.5$, $L = 8$ and: (a) $\Delta = 0$, and (b) $\Delta = 0.5$. Here $\varepsilon^{\rm S}(k)$ $[\varepsilon^{\rm T}(k)]$ denotes spin (orbital) excitation, $\varepsilon^z(k)$ corresponds to an elementary excitation having the same S and T as the ground state, and $\varepsilon^{\rm SO}(k)$ stands for the spin excitation under simultaneous flipping of orbitals.

The phase transition from the dimer phase V to the AS phase III ($S = 0$) appears singular in the sense that it is first order at $\Delta = 0$ and continuous otherwise [figures 5(a,b)]. To locate the center of the continuous phase transition between phases III and V

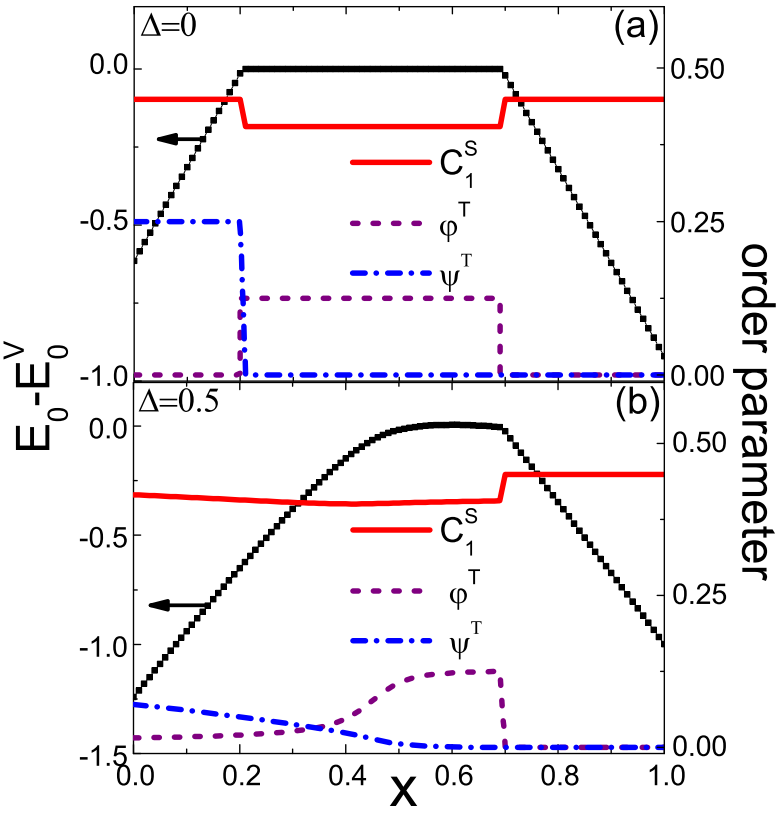

Figure 6. Ground state energy relative to phase V, $E_0(x)-E_0^V(x)$ (dots), orbital order parameters (dashed), $\psi^T = [T^{zz}(\pi)]^{\frac{1}{2}}$, $\varphi^T = [T^{zz}(\pi/2)]^{\frac{1}{2}}$, and bond spin correlations $|S_1| = |\langle \vec{S}_1 \cdot \vec{S}_2 \rangle|$ (solid line), for phases III, V and II (from left to right), for: (a) $\Delta = 0.0$ and (b) $\Delta = 0.5$. Parameters: $y = -0.5$ and $L = 12$.

at $\Delta > 0$, we have selected the peak of the first derivative of the entanglement entropy, see figure 3. Yet also the peaks in the derivatives of the fidelity susceptibility, the orbital correlation function T_1 [see figure 4(b)] and the orbital order parameters ψ^T and φ^T in figure 6(b) may be used. Finally, we note that the scaling of entanglement with system size has quite different behaviour in phases III and V, indicating that a phase transition separates them.

Furthermore, the peculiar feature of the AS/AO phase III manifests itself in a twofold degeneracy and zero SOE at $\Delta = 0$ in contrast to the nondegenerate ground state and finite SOE at finite Δ. The entanglement has two sources, namely: (i) the interplay of quantum fluctuations in the spin and orbital sectors and (ii) the dimerization order which coexists with antiferromagnetic spin correlations in phase III at finite Δ. The latter is the origin of the nondegenerate ground state as it yields a coupling to the $\varepsilon^{\rm SO}(\pi)$ excitation (nearly horizontal in x), and the emergence of the spin-dimer correlations $D(r)$ leads to a faster decay of the spin correlations in phase III than in the 1D antiferromagnetic Heisenberg chain, see the Appendix. The orbital order parameters ψ^T and φ^T compete in phases III and V, see figure 6(b), near the phase boundary in

figure 1(b). This also explains why the transition from phase V to III is smooth at finite Δ in terms of both the vNE (figure 3) and the nearest neighbour spin correlations $|S_1|$.

6. Conclusions and summary

Summarizing, we have studied the quantum phases and the spin-orbital entanglement of the 1D ferromagnetic SU(2)$\otimes XXZ$ model by means of the Lanczos method. We have discovered a previously unknown translational invariant phase V with long-range spin singlet order and four-fold periodicity in the orbital sector. Its mechanism is distinct from the dimer phases found in the 1D antiferromagnetic spin-orbital model near the SU(4) symmetric point [45]. Both III-V and II-V phase transitions arise from the spin-orbital entanglement in the case of Ising orbital interactions. When the orbital interactions change from Ising to anisotropic XXZ-type, the entanglement develops in phase III, where antiferromagnetic spin correlations and long-range spin dimer order coexist, changing the quantum phase transition from first-order to continuous. Furthermore in the regime of finite orbital fluctuations ($\Delta > 0$) another phase VI emerges, which is complementary in many aspects to phase V, but with the important difference that phase VI disappears in the limit $\Delta = 0$.

We have shown that the von Neumann entropy spectral function $\mathcal{S}_{\rm vN}(\omega)$ (2) is a valuable tool that captures the spin-orbital entanglement SOE of excitations and explains the origin of the entanglement entropy change at a phase transition. From the perspective of spin-orbital entanglement we encounter (*i*) first-order transitions between disentangled (II) and entangled (V) phases, (*ii*) a continuous transition involving two competing order parameters between two entangled phases, III and V, and (*iii*) trivial first-order transitions between two disentangled phases. Case (*ii*) goes beyond the commonly accepted paradigm of a single order parameter to characterize a quantum phase.

Moreover, we have presented two simple measures of entanglement in the ground state and shown that they are basically equivalent — the direct measure via the (quartic) spin-orbital bond correlation function C_1 (9) and the von Neumann entropy $\mathcal{S}^0_{\rm vN}$. The latter is defined by separating globally spin from orbital degrees of freedom in the ground state.

Acknowledgments

We thank Bruce Normand and Krzysztof Wohlfeld for insightful discussions. W-L You acknowledges support by the Natural Science Foundation of Jiangsu Province of China under Grant No. BK20141190 and the NSFC under Grant No. 11474211. A M Oleś kindly acknowledges support by Narodowe Centrum Nauki (NCN, National Science Center) under Project No. 2012/04/A/ST3/00331.

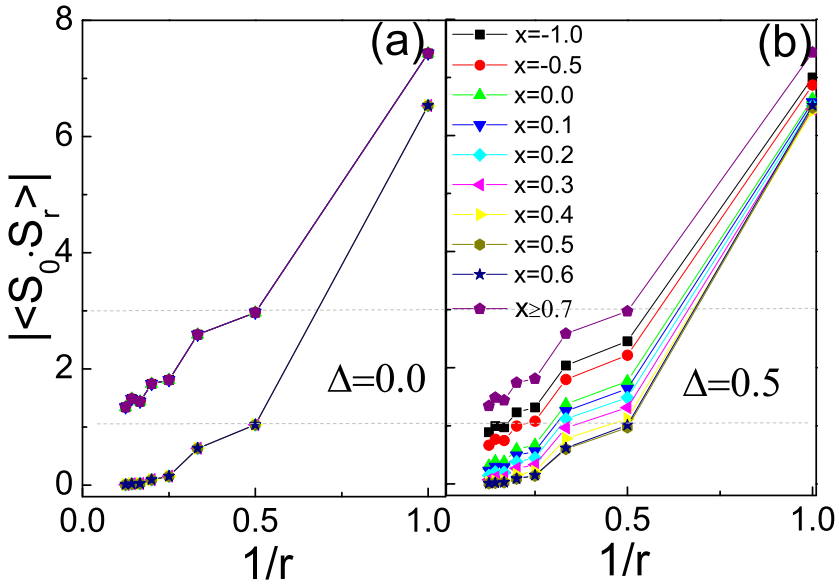

Figure 7. Modulus of spin correlations S_r equation (10) versus the inverse distance $1/r$ as obtained for a spin-orbital ring (3) with $L = 16$ sites, for: (a) $\Delta = 0$, and (b) $\Delta = 0.5$. Parameter: $y = -0.5$.

Appendix: Distance dependence of the antiferromagnetic spin correlations

Here we explore in more detail the competition of the antiferromagnetic (AF) spin correlations of the spin-orbital chain in the AS/AO phase III and the Majumdar-Ghosh like spin-singlet dimer correlations that coexist at finite Δ, as we found in our work. For $\Delta = 0$ the spin correlations in phase III are those of an AF Heisenberg spin chain,

$$\left\langle \vec{S}_i \cdot \vec{S}_{i+r} \right\rangle \sim (-1)^r \frac{\sqrt{\ln |r|}}{|r|}, \tag{12}$$

which reveal the typical $1/r$-power law decay combined with logarithmic corrections that were first predicted by conformal field theory [62,63] as well as by renormalization group methods [64], and subsequently confirmed [65] by numerical density matrix method [66].

In figure 7(a) we present our numerical data for the spin-correlation function S_r equation (10) (i.e., for translational invariant ground states) for several values of x, and for $\Delta = 0$ and $y = -0.5$. In the $\Delta = 0$ case there are only two distinct types of behaviour of S_r, namely exponential decay in phase V and the power law decay of the 1D quantum Néel spin liquid state, which are the same in phases II and III.

Figure 7(b) displays S_r at $\Delta = 0.5$ for different x-values. Here again the unperturbed AF correlations of the 1D Néel spin-liquid state appear in phase II ($x \geq 0.7$). It is evident that in phase III the AF spin correlations are strongly reduced, due to the competition with the coexisting long-range ordered spin-singlet correlations. The spin singlet order increases with x in phase III, and as a consequence we observe here that the decay of S_r becomes stronger as x approaches the III/V transition.

In figure 8 we present a logarithmic plot which highlights the different decays of S_r

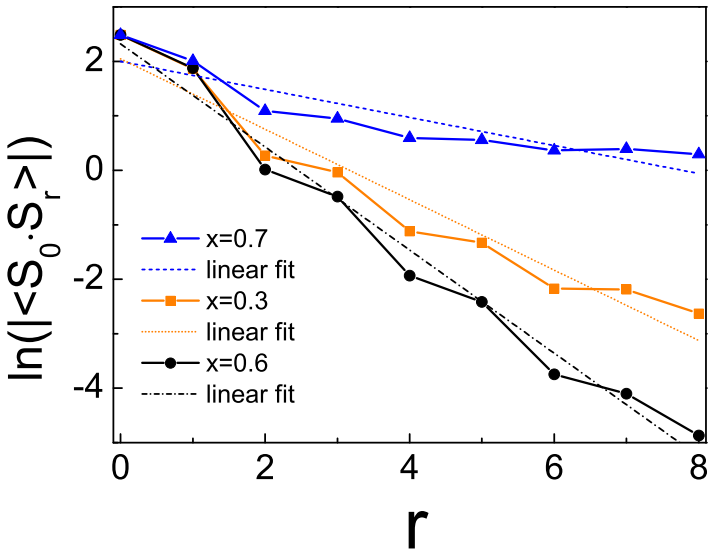

Figure 8. Logarithm of modulus of spin correlations S_r equation (10) for increasing distance r as obtained for the spin-orbital model equation (3) on a ring of $L = 16$ sites for $\Delta = 0.5$, $y = -0.5$, and three values of x. Exponential decay of S_r with increasing r is obtained for phase V ($x = 0.6$).

for $\Delta = 0.5$ in the three different phases: III, V, and II. We have selected the values for $x = 0.3$, 0.6 and 0.7, respectively, for greater transparency. The log-plot shows clearly the exponential decay of S_r in phase V. It also shows that the $L = 16$ system reveals strong finite size effects in phase II where S_r has power law decay. Nevertheless it is clear already from the $L = 16$ data that the AF spin correlations in phase III (here shown for $x = 0.3$) are strongly suppressed and approach the exponential decay of S_r in phase V ($x = 0.5$ and 0.6) when x approaches the III-V phase boundary from the left.

Summarizing, we find that in phase III the AF spin correlations of the 1D Néel spin liquid state decay much more rapidly as the competing spin-singlet order emerges. This effect is particularly strong near the boundary of phase III to the spin-singlet dimer phase V. Whether in the thermodynamic limit the correlations S_r also decay exponentially in phase III as in V cannot be decided here, and this question is beyond the scope of the present work.

References

[1] Kugel K I and Khomskii D I 1973 *JETP* **37** 725
Kugel K I and Khomskii D I 1982 *Sov. Phys. Usp.* **25** 231
[2] Brzezicki W, Oleś A M and Cuoco M 2015 *Phys. Rev. X* **5** 011037
[3] Corboz P, Lajkó M, Läuchli A M, Penc K and Mila F 2012 *Phys. Rev. X* **2** 041013
[4] Tokura Y and Nagaosa N 2000 *Science* **288** 462
[5] Oleś A M, Khaliullin G, Horsch P and Feiner L F 2005 *Phys. Rev. B* **72** 214431
[6] Khaliullin G and Maekawa S 2000 *Phys. Rev. Lett.* **85** 3950

Mochizuki M and Imada M 2004 *New J. Phys.* **6** 154
Pavarini E, Yamasaki A, Nuss J and Andersen O K 2005 *New J. Phys.* **7** 188
[7] Reitsma A, Feiner L F and Oleś A M 2005 *New J. Phys.* **7** 121
[8] Wohlfeld K, Nishimoto S, Haverkort M W and van den Brink J 2013 *Phys. Rev. B* **88** 195138
[9] Solovyev I V 2008 *New J. Phys.* **10** 013035
Wohlfeld K, Daghofer M and Oleś A M 2011 *Europhys. Lett.* **96** 27001
[10] Feiner L F and Oleś A M 1999 *Phys. Rev. B* **59** 3295
[11] Zhou J-S, Ren Y, Yan J-Q, Mitchell J F and Goodenough J B 2008 *Phys. Rev. Lett.* **100** 046401
[12] Khaliullin G 2005 *Prog. Theor. Phys. Suppl.* **160** 155
[13] Horsch P, Oleś A M, Feiner L F and Khaliullin G 2008 *Phys. Rev. Lett.* **100** 167205
[14] Oleś A M, Horsch P, Feiner L F and Khaliullin G 2006 *Phys. Rev. Lett.* **96** 147205
[15] Oleś A M 2012 *J. Phys.: Condens. Matter* **24** 313201
[16] Ulrich U, Khaliullin G, Sirker J, Reehuis M, Ohl M, Miyasaka S, Tokura Y and Keimer B 2003 *Phys. Rev. Lett.* **91** 257202
Horsch P, Khaliullin and Oleś A M 2003 *Phys. Rev. Lett.* **91** 257203
[17] Sirker J, Herzog A, Oleś A M and Horsch P 2008 *Phys. Rev. Lett.* **101** 157204
Herzog A, Horsch P, Oleś A M and Sirker J 2011 *Phys. Rev. B* **83** 245130
[18] Chen C-C, van Veenendaal M, Devereaux T P and Wohlfeld K 2015 *Phys. Rev. B* **91** 165102
[19] Amico L, Fazio R, Osterloh A and Vedral V 2008 *Rev. Mod. Phys.* **80** 517
[20] Zhou H-Q, Barthel T, Fjaerestad J O and Schollwöck U 2006 *Phys. Rev. A* **74** 050305(R)
[21] Byczuk K, Kunes J, Hofstetter W and Vollhardt D 2012 *Phys. Rev. Lett.* **108** 087004
[22] Held K and Mauser N J 2013 *Eur. Phys. J. B* **86** 328
[23] Veenstra C N, Zhu Z-H, Raichle M, Ludbrook B M, Nicolaou A, Slomski B, Landolt G, Kittaka S, Maeno Y, Dil J H, Elfimov I S, Haverkort M W and Damascelli A 2014 *Phys. Rev. Lett.* **112** 127002
[24] Hasan M Z and Kane C L 2010 *Rev. Mod. Phys.* **82** 3045
[25] Jackeli G and Khaliullin G 2009 *Phys. Rev. Lett.* **102** 017205
[26] Gorshkov A V, Hermele M, Gurarie V, Xu C, Julienne P S, Ye J, Zoller P, Demler E, Lukin M D and Rey A M 2010 *Nature Phys.* **6** 289
[27] Mühlbauer S, Binz B, Jonietz F, Pfleiderer C, Rosch A, Neubauer A, Georgii R and Böni P 2009 *Science* **323** 915
[28] Lundgren R, Chua V and Fiete G A 2012 *Phys. Rev. B* **86** 224422
[29] Thomale R, Arovas D P and Bernevig B A 2010 *Phys. Rev. Lett.* **105** 116805
[30] You W-L, Oleś A M and Horsch P 2012 *Phys. Rev. B* **86** 094412
[31] Li H and Haldane F D M 2008 *Phys. Rev. Lett.* **101** 010504
[32] Pollmann F, Turner A M, Berg E and Oshikawa M 2010 *Phys. Rev. B* **81** 064439
Alba V, Haque M and Läuchli A M 2012 *Phys. Rev. Lett.* **108** 227201
[33] Poilblanc D 2010 *Phys. Rev. Lett.* **105** 077202
[34] Fidkowski L 2010 *Phys. Rev. Lett.* **104** 130502
Regnault N and Bernevig B A 2011 *Phys. Rev. X* **1** 021014
[35] Kolley F, Depenbrock S, McCulloch I P, Schollwöck U and Alba V 2013 *Phys. Rev. B* **88** 144426
[36] Lundgren R, Blair J, Greiter M, Läuchli A, Fiete G A and Thomale R 2014 *Phys. Rev. Lett.* **113** 256404
[37] Chandran A, Khemani V and Sondhi S L 2014 *Phys. Rev. Lett.* **113** 060501
[38] Ament L J P, van Veenendaal M, Devereaux T P, Hill J P and van den Brink J 2011 *Rev. Mod. Phys.* **83** 705
[39] Zhao E and Liu W V 2008 *Phys. Rev. Lett.* **100** 160403
Wu C 2008 *Phys. Rev. Lett.* **100** 200406
Wu C and Das Sarma 2008 *Phys. Rev. B* **77** 235107
[40] Sun G, Jackeli G, Santos L and Vekua T 2012 *Phys. Rev. B* **86** 155159
[41] Zhou Z, Zhao E and Liu W V 2015 *Phys. Rev. Lett.* **114** 100406

[42] Li Y-Q, Ma M, Shi D-N and Zhang F-C 1998 *Phys. Rev. Lett.* **81** 3527
Frischmuth B, Mila F and Troyer M 1999 *Phys. Rev. Lett.* **82** 835
[43] Itoi C, Qin S and Affleck I 2000 *Phys. Rev. B* **61** 6747
Orignac E, Citro R and Andrei N 2000 *Phys. Rev. B* **61**, 11533
[44] Yamashita Y, Shibata N and Ueda K 2000 *J. Phys. Soc. Jpn.* **69** 242
[45] Li Peng and Shen Shun-Qing 2005 *Phys. Rev. B* **72** 214439
[46] Kolezhuk A K and Mikeska H-J 1998 *Phys. Rev. Lett.* **80** 2709
[47] Kolezhuk A K, Mikeska H-J and Schollwöck U 2001 *Phys. Rev. B* **63** 064418
[48] Martins M J and Nienhuis B 2000 *Phys. Rev. Lett.* **85** 4956
[49] Kumar B 2013 *Phys. Rev. B* **87** 195105
[50] Brzezicki W, Dziarmaga J and Oleś A M 2014 *Phys. Rev. Lett.* **112** 117204
[51] Belemuk A M, Chtchelkatchev N M and Mikheyenkov A V 2014 *Phys. Rev. A* **90** 023625
[52] You W-L, Li Y-W, and Gu S-J 2007 *Phys. Rev. E* **76** 022101
[53] Yu Y, Müller G and Viswanath V S 1996 *Phys. Rev. B* **54** 9242
[54] Majumdar C K and Ghosh D 1969 *J. Math. Phys.* **10** 1388
[55] Streltsov S V and Khomskii D I 2014 *Phys. Rev. B* **89** 161112(R)
[56] des Cloizeaux J and Pearson J J 1962 *Phys. Rev.* **128** 2131
[57] Horsch P and von der Linden W 1988 *Z. Phys. B* **72** 181
[58] Affleck I 1993 *Rev. Math. Phys.* **6** 887
[59] Koma T and Tasaki H 1994 *J. Stat. Phys.* **76** 745
[60] Spronken G, Fourcade B and Lépine Y 1986 *Phys. Rev. B* **33** 1886
[61] Uhrig G S and Schulz H J 1996 *Phys. Rev. B* **54** R9624
[62] Affleck I, Gepner D, Schulz H and Ziman T 1989 *J. Phys. A: Math. and Theor.* **22** 511
[63] Lukyanov S 1998 *Nuclear Physics B* **522** 533
[64] Giamarchi T and Schulz H J 1989 *Phys. Rev. B* **39** 4620
Singh R R, Fisher M E and Shankar R 1989 *Phys. Rev. B* **39** 2562
[65] Hallberg K A, Horsch P and Martínez G 1995 *Phys. Rev. B* **52** R719
[66] Schollwöck U 2005 *Rev. Mod. Phys.* **77** 259